

Article

# High Intensity Laser Induced Reverse Transfer: Solution for Enhancement of Biocompatibility of Transparent Biomaterials

Naghmeh Safaie <sup>1</sup>, Holly Jones-Taggart <sup>2</sup> and Amirkianoosh Kiani <sup>1,\*</sup> 

<sup>1</sup> Silicon Hall: Micro/Nano Manufacturing Facility, Faculty of Engineering and Applied Science, Ontario Tech University, Oshawa, ON L1G0C5, Canada; Naghmeh.Safaie@uoit.ca

<sup>2</sup> Faculty of Health Sciences, Ontario Tech University, Oshawa, ON L1G0C5, Canada; Holly.JonesTaggart@uoit.ca

\* Correspondence: amirkianoosh.kiani@uoit.ca

Received: 30 August 2019; Accepted: 16 September 2019; Published: 17 September 2019



**Abstract:** Bioactive glass is used extensively in biomedical applications due to its quality and effectiveness in tissue regeneration. Bioactive glasses are able to interact with biological systems and can be used in humans to improve tissue regeneration without any side effects. Bioactive glass is a category of glasses that maintain good contact with body organs and remain biocompatible for a long time after implementation. They have the potential to form a hydroxyapatite surface as a biocompatible layer after immersion in body fluid. In this research, glass biocompatibility was modified using a deposition method called the high intensity laser induced reverse transfer (HILIRT) method and they were utilized as enhanced-biocompatibility bioactive glass (EBBG) with a correspondent nanofibrous titanium (NFTi) coating. HILIRT is a simple ultrafast laser method for improving implants for biomedical applications and provides a good thin film of NFTi on the glass substrate that is compatible with human tissue. The proposed method is a non-chemical method in which NFTi samples with different porosities and biocompatibilities are synthesized at various laser parameters such as power and frequency. Physical properties and cell compatibility and adhesion of these NFTi before and after immersion in simulated body fluid (SBF) were compared. The results indicate that increasing laser intensity and frequency leads to more NFTi fabrication on the glass with no toxicity and better cell interaction and adhesion.

**Keywords:** laser nanofabrication; nano fibrous biomaterials; biocompatibility; transparent materials

## 1. Introduction

Transparent materials such as glass have extensive applications in biomedical science, and since they react with physiological fluids and form tenacious bonds to hard and soft tissues through cellular activity, they have to be compatible with biologic organs and surrounding living tissues [1–5]. Surface modification is one of the methods of changing surface properties such as roughness, absorption, chemistry and the general structure of materials to enhance the biocompatibility without altering material bulk properties [6–9]. Methods used to modify surface properties include chemical, physical and chemophysical treatments like electrochemical etching or photolithography, and these are costly and toxic [6–10]. Another modification process reported previously is to apply an enhanced thin layer on the substrate with a laser without changing the bulk properties [8,11,12]. The primary objective of this research is to compare different parameters of introduced ultrashort pulsed laser processing to enhance the biocompatibility of glass for biomedical use. In this study, nanofibrous titanium (NFTi) on glass substrate was prepared by the high intensity laser induced reverse transfer

(HILIRT) method and compared with theoretical results of the process. In this method, high laser energy passes through the transparent glass slides, which is then focused to a very small point on the titanium sheet (target material) in a picosecond range with different laser intensities and pulse intervals. Removing titanium particles from a titanium sheet and accumulating them as nanofibers on the glass surface is the result of the energy input from the laser being absorbed and causing the solid's binding energy to be broken [11–13]. This classic method increases atomic kinetic energy and temperature and finally causes phase transitions. Unlike other heating methods, the focused laser beam primarily impacts a material's electrons in a short time scale [13,14]. When the laser is centralized on a surface, it causes material ablation and removes atoms from the bulk surface, thus enabling these atoms to be emitted and form plasma plume, consequently generating nanofibrous structures by rapid cooling [14]. In this study we investigated the effect of laser power and laser frequency on deposited nanofibrous titanium (NFTi) thin film and biocompatibility on glass substrates via the HILIRT method. In order to analyze the deposited titanium and enhanced-biocompatibility bioactive glass (EBBG) structures and morphologies, a scanning electron microscope (SEM) was used. X-ray diffraction (XRD), and Raman spectroscopy were utilized for structural identification of deposited titanium coatings and hydroxyapatite-like layers formed on EBBG. To assess biocompatibility, an MTT metabolic activity assay was used to determine human cell viability on these substrates.

## 2. Experimental Methods

### 2.1. Fabrication Procedure and Materials

A picosecond laser beam was scanned over the microscope slide and Grade 4 titanium substrate and caused the ablated materials (Ti and Ti oxide) to be deposited on the glass substrate in the form of nanofibers. The general configuration for HILIRT process has been described in detail before [12]. In this research, the laser system used to transfer material from a Ti sheet (Titanium CP3–Grade 4: Commercially Pure Titanium Grade 4) to the glass substrate (Plain Glass Microscope Slides by Fisherbrand™ (Fisher Scientific, Hampton, NH, USA) with thickness of 1 mm) was a Ytterbium pulsed fiber laser (IPG Laser Model: YLPP-1-150V30, IPG Photonics, Oxford, MA, USA) with a wavelength of 1064 nm, at 150 picosecond pulse duration, a pitch of 0.025 mm and scanning speed of 100 mm/s under ambient conditions. The tests were performed with laser powers ranging from 5 to 12 W and laser frequencies ranging from 600 to 1200 kHz. MarkingMate 1.0 software (Eastern Logic Inc.) was used for changing laser parameters such as power and frequency.

### 2.2. Theoretical Methods

The simulation of the ablation process for different ranges of laser powers and pulse repetitions (two main laser parameters) was conducted using an analytical model in MATLAB R2015b software (9.6.0.1072779). In this research, the variable ranges of frequency and power were chosen according to the laser system functionality, from 600 to 1200 kHz and from 5 to 12 W, respectively.

In the theoretical model, the 3D radial temperature gradient can be estimated by Equation (1), in which titanium diffusivity is shown as  $k$ ; where  $r$  and  $z$  are the radius of laser spot and the depth of the laser heat affected zone, respectively, and  $K$  is titanium thermal conductivity [15].

$$\Delta T(r, z, \tau) = \frac{I_{\max} \gamma \sqrt{k}}{\sqrt{\pi} K} \int_0^{\tau} \frac{p(\tau - t)}{\sqrt{t \left[ 1 + \frac{8kt}{W^2} \right]}} e^{-\left[ \frac{z^2}{4kt} + \frac{r^2}{4kt + 0.5W^2} \right]} dt \quad (1)$$

Here,  $I_{\max}$  is the peak intensity, and  $W$  is the beam's (1/e) field radius. Also,  $p(t)$  is related to the pulse shape and we assume we have square-shaped pulses. Additionally, the ablation depth,  $h(r)$ , as a function of a radial position from the center of the focused laser beam spot, can be anticipated by Equation (2) [15–17]:

$$h(r) = \sqrt{-4\beta k\tau \ln\left\{\frac{\beta K\Delta T_B}{\gamma I_{\max}} \sqrt{\frac{\pi}{k\beta\tau}} \left(1 + \frac{8\beta k\tau}{W^2}\right)\right\}} - \frac{r^2}{1 + \frac{W^2}{8\beta k\tau}} \leq h(0) \quad (2)$$

In Equation (2),  $\Delta T_B$  is equal to  $T_{\text{boiling}} - T_{\text{room}}$  temperature and  $\beta$  has the constant value of 0.5 for considered pulse duration,  $R$  is titanium Fresnel energy reflectivity,  $\gamma$  is a fraction of pulse energy absorbed by titanium, and  $W$  is the beam's field radius [12,15].

### 2.3. Characterization Procedure

In order to analyze the deposited Ti structures and the hydroxyapatite and other calcium to phosphorus composition characterizations on the prepared Ti glass after soaking for 4 days in simulated body fluid (SBF), a SEM (Quanta 3D by Thermo Fisher, Hillsboro, OR, USA) was used. SBF is a solution with similar ions to those existing in human body and a similar ion concentration to human blood plasma, and was prepared in this research by following Kokubo and Takadama [5]. Recognizing fiber diameters was done through 1.501 ImageJ software using SEM images. SEM was also used to see the MT3 cell cytoskeletons and their adhesion on different produced samples. A Rigaku Ultima IV X-ray diffractometer (Tokyo, Japan) with Cu K $\alpha$  radiation ( $\lambda = 0.15418$  nm), and a Renishaw Raman spectrometer (Wotton-under-Edge, UK) were used for the structural identification of deposited titanium coatings and different hydroxyapatite compositions on them.

### 2.4. MTT Assay

In this research, a colorimetric metabolic activity (MTT) assay was done in order to indirectly study the viability of human cells on NFTi coated glass before and after immersion in SBF. The MTT assay was performed on 10,000 HT-29 cells incubated in media solution exposed to NFTi coated glass for 2, 4 and 6 days. After cell exposure to this media, cells were washed with phosphate buffered solution (PBS) and incubated with a fresh serum-free medium containing dye compound 3-(4,5-dimethylthiazol-2-yl)-2,5-diphenyltetrazolium bromide (MTT reagent) in a dark 37 °C, 5% CO<sub>2</sub> humidified incubator for 4 h. Finally, the resulting colored solution was measured by absorbance at 500–600 nm wavelength using a multi-well spectrophotometer. Results are presented as a percentage of treated cells that remained viable compared to non-treated cells (%).

### 2.5. Cell Adhesion

Adhesion to specimens has a remarkable effect on the proliferation and differentiation of cells. To investigate cell adhesion on synthesized NFTi coatings, 10<sup>4</sup> human epithelial cells from the HT-29 cell line were seeded on samples which were sterilized with 70% alcohol in cell cultures and incubated with 5% CO<sub>2</sub> in 37 °C for 72 h. After incubation, the samples were washed with PBS to remove non-adherent and dead cells. Samples with adherent cells were fixed with 2.5 vol.% fixative glutaraldehyde solutions and incubated for 1 h. The specimens were washed twice with PBS to remove the glutaraldehyde that remained, and subsequently samples were rinsed with 30%, 50%, 70%, 90% and 100% absolute ethanol for 15 min and were taken to the SEM lab for further investigation.

## 3. Results and Discussion

As illustrated in Figure 1, by increasing laser power from 5 to 12 W, the amount of NFTi increased. It is also clear that a laser power of 5 W is not enough laser intensity for removing particles and ablating materials, since the surface of the microscope glass that went through laser deposition with a laser power of 5 W was similar to bare glass, with only a small amount of NFTi. This means that when a laser power of 5 W was focused over a glass surface, it raised the temperature, but not high enough to produce sufficient material ablation and remove atoms and particles from the bulk surface; therefore, the titanium atoms could not be emitted from the titanium sheet and small amount of nanofibers could be formed via rapid cooling process (Figure 1A). Also, since by increasing laser power the shape of

deposited materials would change from agglomerated to nanostructure, their diameter decreased, which is shown in Figure 1D. As shown in Figure 1 and as reported before [9,12], the surface roughness in microscale has not been changed significantly.

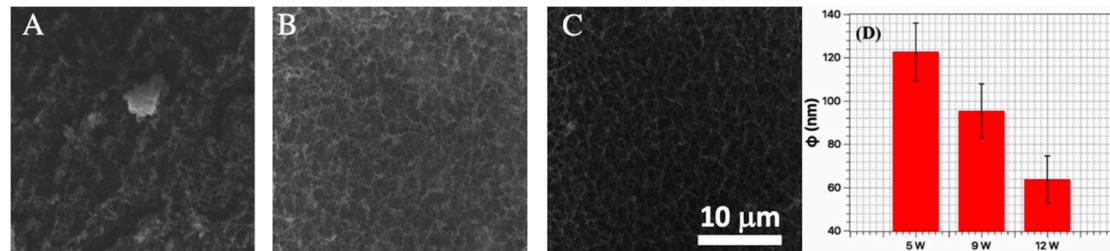


**Figure 1.** Scanning electron microscope (SEM) images of (A) nanofibrous titanium (NFTi) deposited layer on glass with laser power of 5 W; (B) NFTi deposited layer on glass with laser power of 9 W; and (C) NFTi deposited layer on glass with laser power of 12 W; (D) Column chart of fiber diameters by increased laser power.

As per Equation (1), the radial temperature gradient has a direct relation to the  $I_{\max}$  which is directly dependent on the average laser power. This means that by increasing the laser power, the temperature gradient goes up and a larger HAZ forms, as shown in Figure 2.

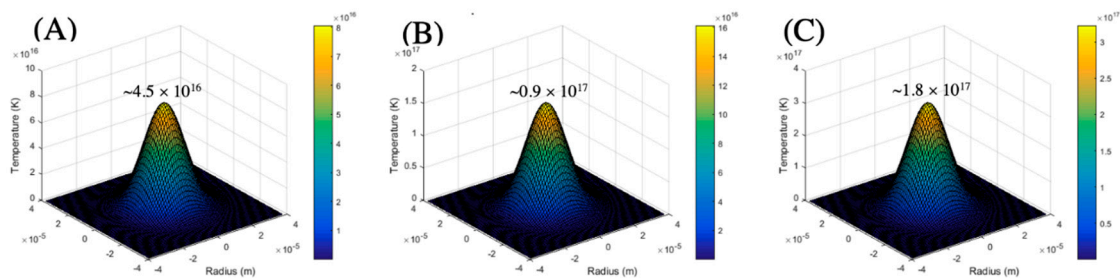


**Figure 2.** The 3D radial temperature gradient profiles for laser power of (A) 5 W; (B) 9 W and (C) 12 W.

As displayed in Figure 3, by increasing the laser power and decreasing the scanning speed, the ablation depth increases. To further clarify, incrementing laser power while other laser parameters are constant causes the amount of the energy delivered to the Ti substrate to increase. This results in the generation of a larger HAZ and greater ablation volume on the Ti surface, which is in agreement with the results presented in Figure 2. The laser scanning speed has a similar behavior, as at lower scanning speed (higher number of pulses) more energy would be transferred to the substrate, which results in a deeper ablation profile and thicker nanofibrous layer.

The effect of laser frequency is shown in Figure 4. By increasing laser frequency from 600 to 1200 kHz, the amount of NFTi also increased. This can be due to the fact that increasing laser frequency means decreasing pulse intervals, which leads to a shorter time between consecutive pulses and more transmitted intensity into the substrate, and more heat accumulation and higher average temperature [15–19]. Enhancing the spot temperature causes a denser plume and generates more ablated atoms, thus leading to more consecutive inelastic collisions, which results in the deposition of a titanium nanostructure on glass substrates with reduced diameter [15].

In the HILIRT method, the effect of pulse repetition needs to be considered along with the number of delivered laser pulses. Generally, at a higher pulse repetition rate and a constant amount of average laser power, the energy of each pulse is less, which leads to the lower maximum temperature for the HAZ, as demonstrated in Figure 5. However, for multi-pulse processes, the average surface temperature increases by increasing the pulse repetition [15–18]. Increasing the laser repetition rate

results in decreased pulse intervals (shorter time between consecutive pulses) and a higher number of laser pulses per unit time (delivering more laser intensity into the substrate) [15–18].

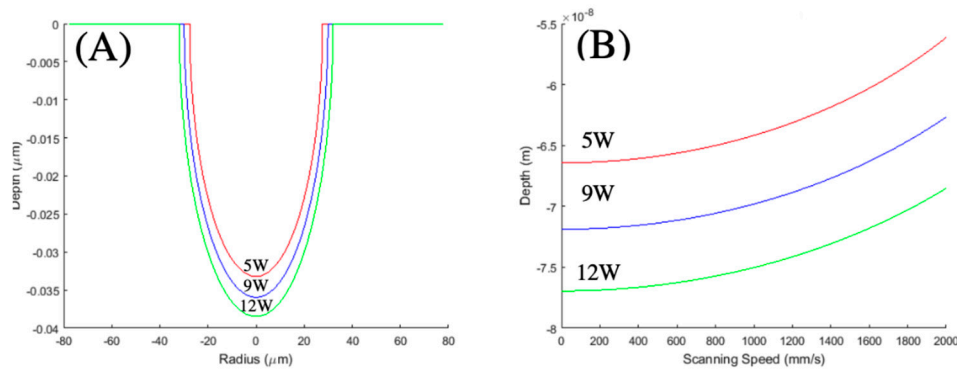


**Figure 3.** (A) Theoretical ablation depth profile as a function of radius and (B) theoretical ablation depth profile as a function of laser scanning speed for single pulsed laser with powers of 5, 9 and 12 W.

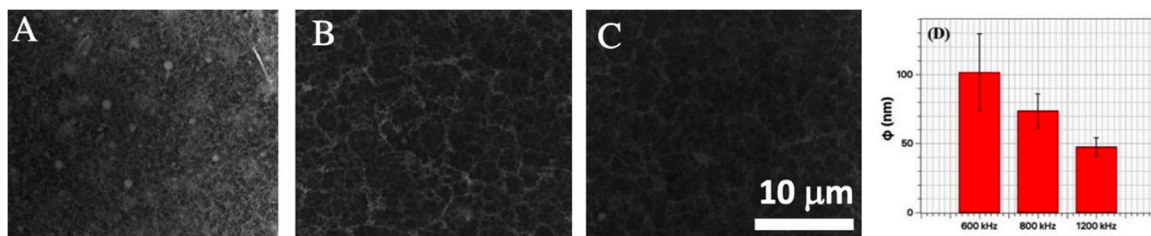


**Figure 4.** SEM images of (A) NFTi deposited layer on glass with laser frequency of 600 kHz; (B) NFTi deposited layer on glass with laser frequency of 800 kHz and (C) NFTi deposited layer on glass with laser frequency of 1200 kHz; (D) Column chart of fiber diameters by increasing laser frequency.

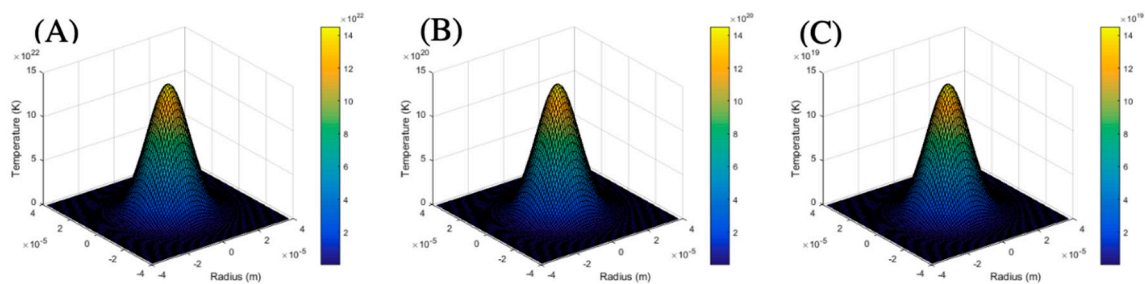


**Figure 5.** The 3D temperature gradient profile for (A) laser frequency of 600 kHz; (B) laser frequency of 800 kHz; and (C) laser frequency of 1200 kHz.

As stated in the above paragraph, at higher laser repetition rates and shorter pulse intervals, denser laser plumes would be formed as the average surface temperature is higher [15,18]; this causes the generation of smaller laser ablation volume (and more fibers) as shown in Figure 6.

The ability to form the hydroxyapatite layer with a calcium to phosphorous ratio of 1.63 and other compositions of these two elements is known as biocompatibility [4]. In order to analyze the specimens' biocompatibility, samples should be immersed in SBF. All the specimens produced with different laser powers and frequencies were immersed in SBF for 4 days, and the SEM results show the hydroxyapatite-like layer, which is a good indication of the samples' biocompatibility. Additionally, increasing laser power and frequency creates better and more consistent layers of hydroxyapatite which can be the result of more NFTi on the samples. To illustrate further, samples with more NFTi have greater area to volume ratio of suitable places for calcium and phosphorous to nucleate and grow on, which means that they have more biocompatible surfaces, as indicated in Figures 7 and 8.

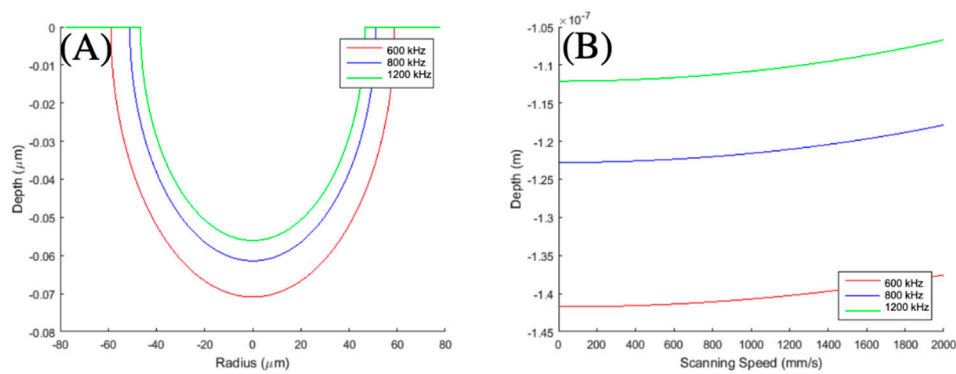


**Figure 6.** (A) Theoretical ablation depth profile as a function of radius and (B) theoretical ablation depth profile as a function of laser scanning speed for single pulsed laser with frequency of 600, 800 and 1200 kHz.

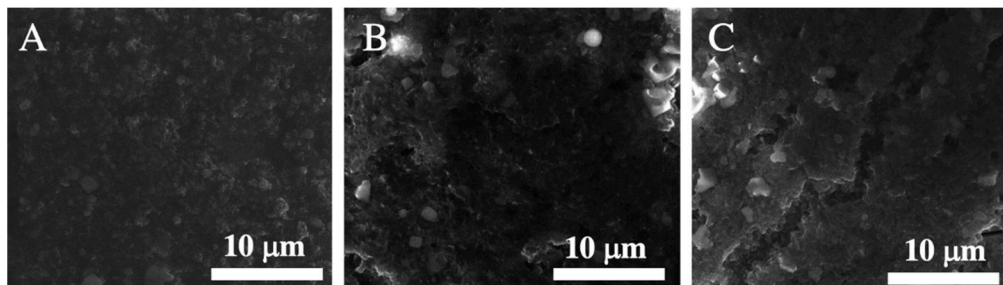


**Figure 7.** SEM images of samples after immersion in simulated body fluid (SBF) solution. (A) Produced by laser power of 5 W and immersed in SBF for 4 days; (B) produced by laser power of 9 W and immersed in SBF for 4 days and (C) produced by laser power of 12 W and immersed in SBF for 4 days.

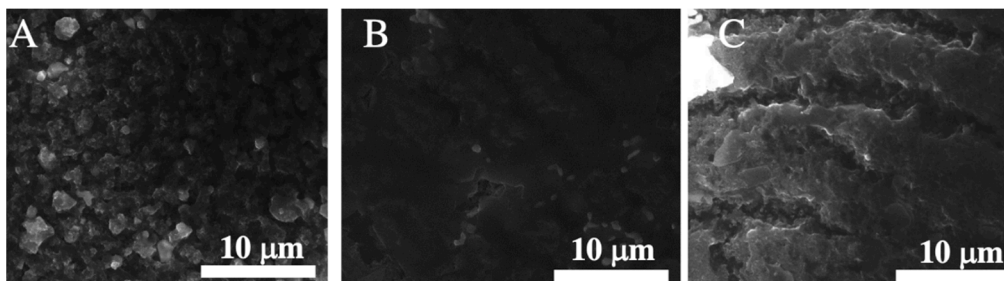


**Figure 8.** SEM images of samples after immersion in SBF solution. (A) Produced by laser frequency of 600 kHz and immersed in SBF for 4 days; (B) produced by laser frequency of 800 kHz and immersed in SBF for 4 days and (C) produced by laser frequency of 1200 kHz and immersed in SBF for 4 days.

The XRD and Raman results in Figure 9 show that titanium and titanium oxide phases reflected severe peaks on samples created by laser powers of 5, 9 and 12 W. Generally, increasing laser power results in injecting pulses with higher intensity on the center of the ablation, which leads to a rise in the plume temperature and consequently more particle ablation and fiber generation.

In samples that were immersed in SBF solution for 4 days according to the previous reported results for similar structures [9,12] there are primary peaks related to hydroxyapatite-like composition, which can be the result of a good amount of NFTi on the samples and proper places for calcium and phosphorous to grow on, as shown in Figure 10. The hydroxyapatite and other calcium to phosphorus composition peaks relating to Raman and XRD patterns of samples which were produced by higher powers have higher intensities compared to the samples produced by a laser power of 5 W. This can

also be due to little or no generation of NFTi on the specimens produced by a laser power of 5 W, and less suitable places where calcium and phosphorous elements can start nucleating and growing [20,21].

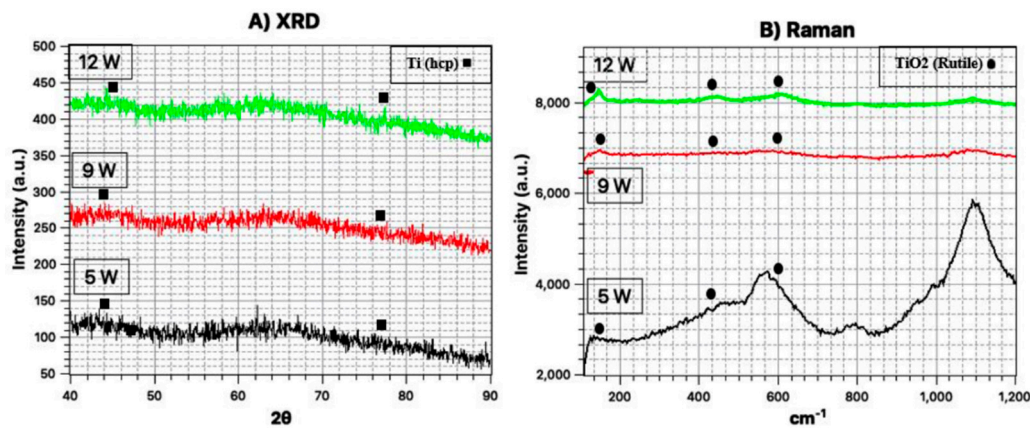


**Figure 9.** (A) X-ray diffraction (XRD) pattern and (B) Raman spectrum of glass samples coated by titanium with different laser powers.

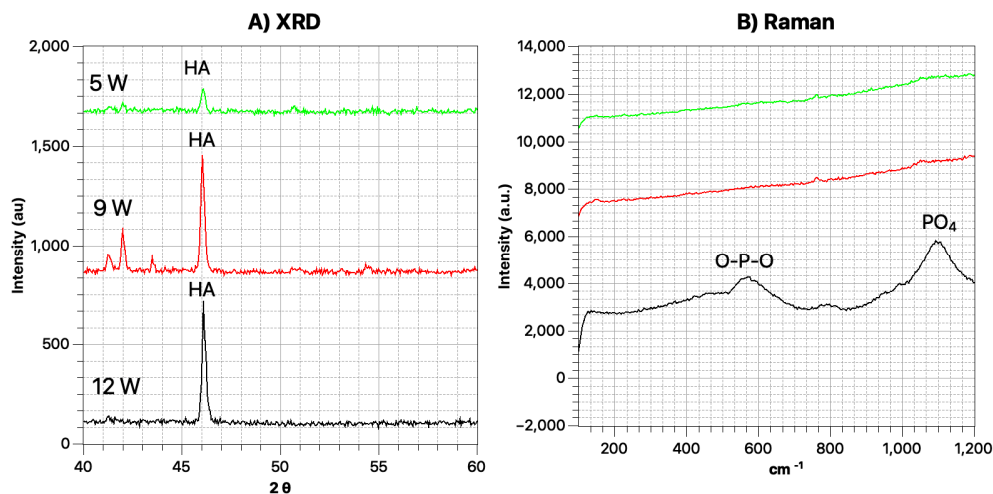


**Figure 10.** (A) XRD pattern and (B) Raman spectrum of glass samples coated by titanium with different laser powers after 4 days immersion in SBF.

The XRD and Raman results in Figure 11 show that titanium and titanium oxide phases reflected severe peaks on samples created by laser frequencies of 600, 800 and 1200 kHz. Generally, increasing laser frequency means a decrease in the laser pulse interval, which brings about a rise in plume temperature and consequently more particle ablations and more fiber generation.

Also, in samples immersed in SBF solution there are several peaks related to hydroxyapatite-like layers which are the result of a good amount of NFTi on the samples and good places for calcium and phosphorous to develop. As illustrated in Figure 12, the hydroxyapatite and other calcium to phosphorus composition peaks relating to Raman and XRD patterns of samples produced by higher laser frequencies have higher intensities compared to the sample produced by a laser frequency of 600 kHz. This can be due to little or insufficient generation of NFTi on the sample produced by the laser frequency of 600 kHz, and less desirable places for calcium and phosphorous elements to start growing. Also, similar to laser power, the sample produced with the highest laser frequency has a drastic upper shift in the Raman spectrum which can be due to the thicker NFTi coating generation.

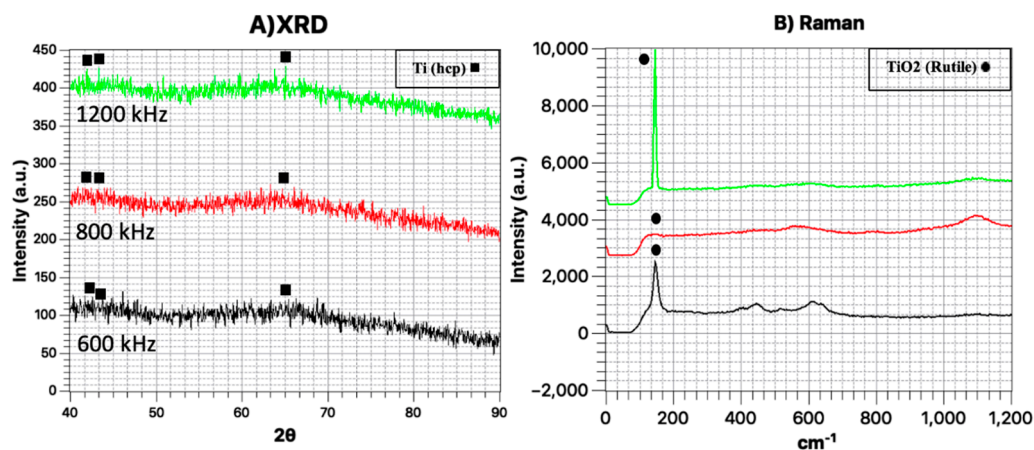


**Figure 11.** (A) XRD pattern and (B) Raman spectrum of glass samples coated by titanium with different laser frequencies.

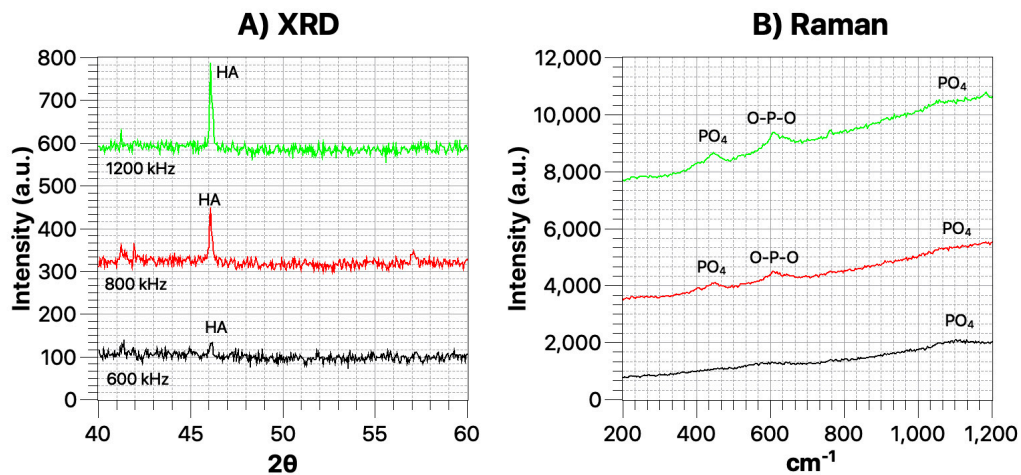


**Figure 12.** (A) XRD pattern and (B) Raman spectrum of glass samples coated by titanium with different laser frequencies after 4 days immersion in SBF.

Indirect MTT assay of the produced samples is shown in Figure 13. Generally, samples with different NFTi coatings did not show high toxicity after three days. Cell viability was constant at 100% over the period due to no toxic ion release into the test solution and no significant effect on its life properties. Although there is no difference between the cell viability of the samples produced with different laser frequencies (almost 100% viability), the solution extracted from the sample produced with a laser power of 5 W showed insignificant toxicity after immersion for 2 and 4 days in the medium. This can be representative of insufficient or less NFTi generation on the glass and no protective or compatible titanium and hydroxyapatite-like layers on top of the glass substrate to prevent toxic ion release, such as silicon ions, from the glass substrate [20,21].

SEM images of cell morphology and cell adhesion on samples with different laser parameters are shown in Figure 14. Attached cells on samples produced with a laser power of 5 W and a laser frequency of 600 kHz can be seen in Figure 14, in comparison with samples synthesized with higher laser powers and higher laser frequencies. The SEM results illustrate that cells adhered better on NFTi surface than bare glass and they are attached better and seem healthier at higher power and higher frequency samples. This can show the biocompatibility of NFTi on the coating produced with higher frequencies and the preference of cells to be fitted on an NFTi coating rather than bare glass. Additionally, cell filopodia have more attachments on the NFTi layers, which is known as their extra cellular matrix (ECM), with increasing laser power and frequency. Cell bodies show less degradation and disappearance during the fixing process, which means that increasing laser power and frequency brings about more NFTi generation and thicker NFTi layers on glass substrate, with higher surface

to volume ratio and more compatible and available places as ECM for cell filopodia to connect and adhere to [21].

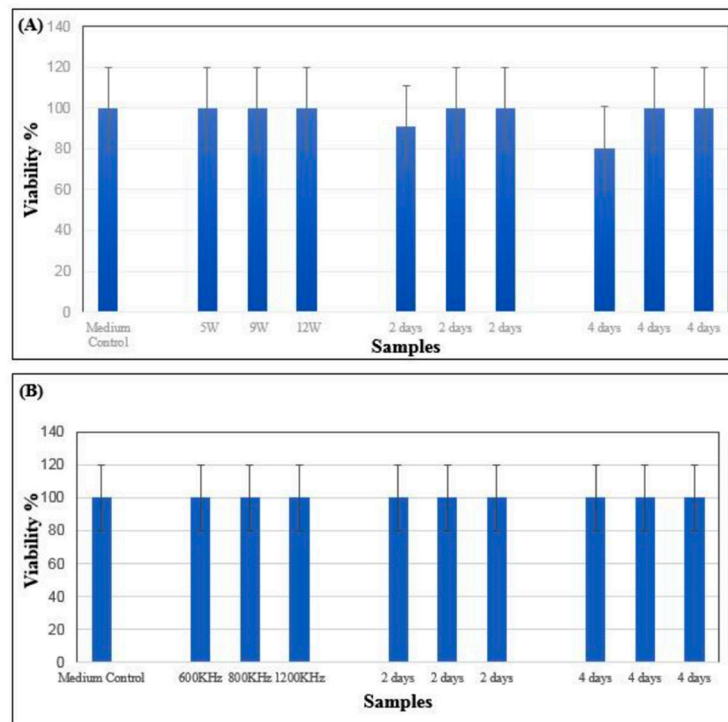


**Figure 13.** (A) MTT results of samples produced with different laser powers before and after immersion in SBF; (B) MTT results of samples produced with different laser frequencies before and after immersion in SBF.

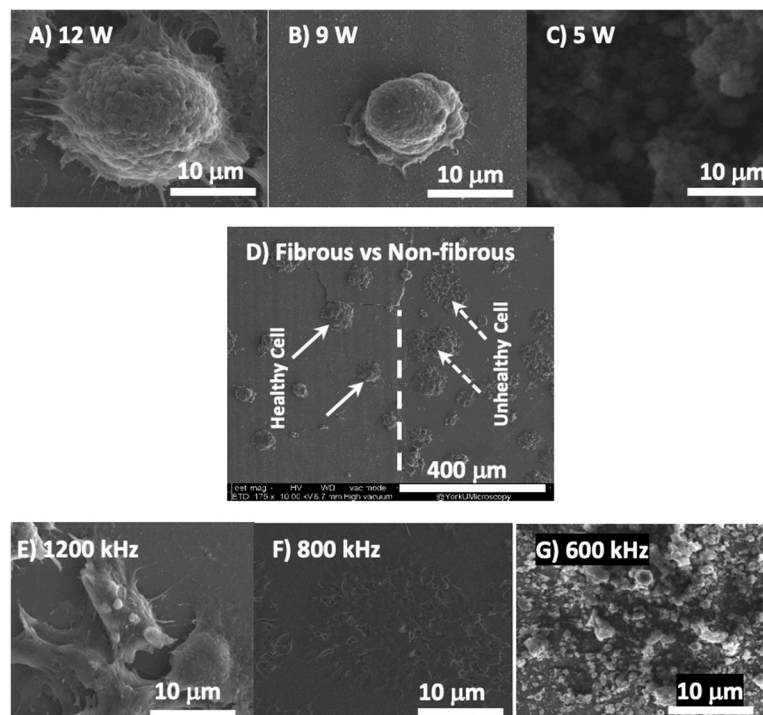


**Figure 14.** SEM images of cells attached on the surface of samples produced with laser power of (A) 12 W; (B) 9 W and (C) 5 W; (D) SEM images of cells attached on the mutual NFTi surface and glass border of samples produced with laser frequency of 1200 kHz. SEM images of cells attached on the surface of samples produced with laser frequency of (E) 1200 kHz; (F) 800 kHz; and (G) 600 kHz.

#### 4. Conclusions

In this research, we presented a new approach for the surface modification of biomaterials in tissue engineering applications. With this method, which is called high intensity laser induced reverse transfer method (HILIRT), we can provide a thin film of titanium nanofibers coated on glass surfaces to be used in a variety of biomedical applications. We investigated the effect of laser power and frequency on a generated nanofibrous titanium (NFTi) structure to achieve high surface biocompatibility and enhance the in vitro cell–material adhesion. Results show that higher laser power and frequency elevate the formation of NFTi, resulting in more deposited hydroxyapatite-like layers on the desired surface of NFTi and more biocompatibility after immersion in simulated body fluid (SBF). Our biological results of high cell viability and cell adhesion indicate that the NFTi coatings produced with a higher laser frequency and higher laser power have better biocompatibility and more desirable surface areas for cells to be absorbed. We believe that the proposed HILIRT method can be an efficient and time-saving laser procedure for fabrication of a wide range of transparent and glassy scaffolds and implants in tissue engineering applications. Theoretical results show that the increasing of laser power leads to the formation of a larger HAZ and higher ablation rates. Also, increasing the laser repetition rate results in decreased maximum temperature for a single laser pulse; however, it brings about more ablated materials with higher accumulated temperatures because of a higher number of pulses and shorter pulse intervals, which leads to higher average surface temperature.

**Author Contributions:** Conceptualization, A.K.; Methodology, A.K. and N.S.; Validation, A.K. and H.J.-T.; Formal Analysis, A.K. and N.S.; Investigation, N.S.; Resources, A.K.; Data Curation, A.K.; Writing–Original Draft Preparation, N.S.; Writing–Review and Editing, A.K. and H.J.-T.; Visualization, A.K. and N.S.; Supervision, A.K.; Project Administration, A.K.; Funding Acquisition, A.K.

**Funding:** This research was funded by the National Sciences and Engineering Research Council (NSERC) Discovery Grant program (RGPIN-2015-05450).

**Conflicts of Interest:** The authors declare no conflict of interest.

#### References

1. Chen, F.M.; Liu, X. Advancing biomaterials of human origin for tissue engineering. *Prog. Polym. Sci.* **2016**, *53*, 86–168. [[CrossRef](#)] [[PubMed](#)]
2. Williams, D.F. *Definitions in Biomaterials: Proceedings of a Consensus Conference of the European Society for Biomaterials, Chester, England, 3–5 March 1986*; Williams, D.F., Ed.; Elsevier Science Limited: Amsterdam, The Netherlands, 1987; Volume 4.
3. Rahaman, M.N.; Day, D.E.; Bal, B.S.; Fu, Q.; Jung, S.B.; Bonewald, L.F.; Tomsia, A.P. Bioactive glass in tissue engineering. *Acta Biomater.* **2011**, *7*, 2355–2373. [[CrossRef](#)] [[PubMed](#)]
4. Kokubo, T.; Kushitani, H.; Sakka, S.; Kitsugi, T.; Yamamuro, T. Solutions able to reproduce in vivo surface-structure changes in bioactive glass-ceramic A-W3. *J. Biomed. Mater. Res. Part A* **1990**, *24*, 721–734. [[CrossRef](#)] [[PubMed](#)]
5. Kokubo, T.; Takadama, H. How useful is SBF in predicting in vivo bone bioactivity? *Biomaterials* **2006**, *27*, 2907–2915. [[CrossRef](#)] [[PubMed](#)]
6. Jones, M.H.; Jones, S.H. *Wet-Chemical Etching and Cleaning of Silicon*; Virginia Semiconductor: Fredericksburg, VA, USA, 2003.
7. Buckberry, L.; Bayliss, S. Porous silicon as a biomaterial. *Mater. World* **1999**, *7*, 213–215.
8. Dhanekar, S.; Jain, S. Porous silicon biosensor: Current status. *Biosens. Bioelectron.* **2013**, *41*, 54–64. [[CrossRef](#)] [[PubMed](#)]
9. Colpitts, C.; Ektesabi, A.M.; Wyatt, R.A.; Crawford, B.D.; Kiani, A. Mammalian fibroblast cells show strong preference for laser-generated hybrid amorphous silicon-SiO<sub>2</sub> textures. *J. Appl. Biomater. Funct. Mater.* **2017**, *15*, 84–92. [[CrossRef](#)] [[PubMed](#)]
10. Qiu, Z.Y.; Chen, C.; Wang, X.M.; Lee, I.S. Advances in the surface modification techniques of bone-related implants for last 10 years. *Regen. Biomater.* **2014**, *1*, 67–79. [[CrossRef](#)] [[PubMed](#)]

11. Kiani, A.; Venkatakrisnan, K.; Tan, B. Micro/nano scale amorphization of silicon by femtosecond laser irradiation. *Opt. Express* **2009**, *17*, 16518–16526. [[CrossRef](#)] [[PubMed](#)]
12. Safaie, N.; Kiani, A. Enhancement of bioactivity of glass by deposition of nanofibrous Ti using high intensity laser induced reverse transfer method. *Vacuum* **2018**, *157*, 92–99. [[CrossRef](#)]
13. Reif, J. Basic Physics of Femtosecond Laser Ablation. In *Laser-Surface Interactions for New Materials Production*; Springer: Berlin/Heidelberg, Germany, 2010; pp. 19–41.
14. Shruthi, G.S.; Amitha, C.V.; Mathew, B.B. Biosensors: A modern-day achievement. *J. Instrum. Technol.* **2014**, *2*, 26–39.
15. Hendow, S.T.; Shakir, S.A. Structuring materials with nanosecond laser pulses. *Opt. Express* **2010**, *18*, 10188–10199. [[CrossRef](#)] [[PubMed](#)]
16. Paladiya, C.; Kiani, A. Synthesis of silicon nano-fibrous (SiNf) thin film with controlled thickness and electrical resistivity. *Results Phys.* **2019**, *12*, 1319–1328. [[CrossRef](#)]
17. Colpitts, C.; Kiani, A. Laser processing of silicon for synthesis of better biomaterials. *Biomater. Regen. Med.* **2018**, *4*, 229.
18. Gamaly, E.G.; Rode, A.V.; Luther-Davies, B. Ultrafast ablation with high-pulse-rate lasers. Part I: Theoretical considerations. *J. Appl. Phys.* **1999**, *85*, 4213–4221. [[CrossRef](#)]
19. Hamza, S.; Ignaszak, A.; Kiani, A. Synthesis of electrical conductive silica nanofiber/gold nanoparticle composite by laser pulses and sputtering technique. *Nanoscale Res. Lett.* **2017**, *12*, 432. [[CrossRef](#)] [[PubMed](#)]
20. Kiani, A.; Venkatakrisnan, K.; Tan, B. Direct laser writing of amorphous silicon on Si-substrate induced by high repetition femtosecond pulses. *J. Appl. Phys.* **2010**, *108*, 074907. [[CrossRef](#)]
21. Bagha, P.S.; Khakbiz, M.; Safaie, N.; Sheibani, S.; Ebrahimi-Barough, S. Effect of high energy ball milling on the properties of biodegradable nanostructured Fe-35 wt.% Mn alloy. *J. Alloy. Compd.* **2018**, *768*, 166–175. [[CrossRef](#)]



© 2019 by the authors. Licensee MDPI, Basel, Switzerland. This article is an open access article distributed under the terms and conditions of the Creative Commons Attribution (CC BY) license (<http://creativecommons.org/licenses/by/4.0/>).